

Graph Partitioning into Hamiltonian Subgraphs on a Quantum Annealer

Eugenio Cocchi,¹ Edoardo Tignone,¹ and Davide Vodola^{1,2,3}

¹Quantum Glare Ltd, London, United Kingdom

²Dipartimento di Fisica e Astronomia dell'Università di Bologna, I-40127 Bologna, Italy

³INFN, Sezione di Bologna, I-40127 Bologna, Italy

We demonstrate that a quantum annealer can be used to solve the NP-complete problem of graph partitioning into subgraphs containing Hamiltonian cycles of constrained length. We present a method to find a partition of a given directed graph into Hamiltonian subgraphs with three or more vertices, called vertex 3-cycle cover. We formulate the problem as a quadratic unconstrained binary optimisation and run it on a D-Wave Advantage quantum annealer. We test our method on synthetic graphs constructed by adding a number of random edges to a set of disjoint cycles. We show that the probability of solution is independent of the cycle length, and a solution is found for graphs up to 4000 vertices and 5200 edges, close to the number of physical working qubits available on the quantum annealer.

I. INTRODUCTION

Many combinatorial optimisation problems arising in practical applications are notoriously hard to solve with classical methods [1]. Recently, quantum annealers have been considered as potentially faster alternatives for finding solutions to this class of problems in different domains. For example, in logistics they have been employed for job shop scheduling [2], traffic flow optimisation [3–5], and airport gate assignment [6]. In telecommunications quantum annealers have been used for satellite coverage [7], and in chemistry for protein folding [8]. In finance, use cases range from portfolio optimisation [9, 10] to prediction of financial crashes [11].

Finding Hamiltonian cycles, i.e. cycles that visit each vertex exactly once, is another type of combinatorial optimisation problem having several applications, for example in kidney and lung exchange [12–14], house allocation [15], branch selection for cadets [16], and, more generally, good exchange [17]. However, so far quantum annealers have not been used to solve these problems. Here, we consider the partitioning of a directed graph into subgraphs containing Hamiltonian cycles. More specifically, we focus on the case where the cycle length is required to be at least three, which makes the problem NP-complete [1]. This problem is also known as the vertex 3-cycle cover decision problem for directed graphs (3-DCC) [18].

For solving the problem on the quantum annealer, we cast its cost function and the corresponding constraints as a Quadratic Unconstrained Binary Optimisation (QUBO) problem. We consider graphs containing disjoint cycles and random edges added and we analyse the probability of finding a vertex 3-cycle cover in a single run on the quantum annealer as a function of the size of the input graph as well as the number of edges added. We find solutions for input graphs up to 4000 vertices and 5200 edges, close to the number of physical working qubits available on the quantum annealer. We find that the dependence of the probability on the system size is stronger when the relative number of random edges added is higher, while it does not depend on the

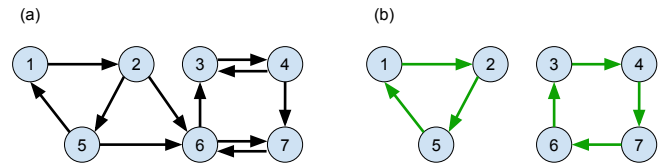


FIG. 1. **Partitioning of a directed graph into Hamiltonian subgraphs.** (a) A directed graph is defined by a set of vertices (circles), connected by directed edges (black arrows). (b) A NP-complete version of the problem of partitioning a directed graph into Hamiltonian subgraphs consists in choosing the right edges (green arrows) in order to form cycles of length greater than or equal to three, without leaving any vertices unconnected.

length of the cycles in the input graph.

This paper is structured as follows. In Sec. II we introduce the relevant definitions and formally define the problem. In Sec. III we show the procedure used to rewrite the problem as a QUBO. In Sec. IV we describe the quantum annealing protocol and the procedure used to test the solutions found. In Sec. V we present the results obtained with D-Wave Advantage quantum annealer. In Sec. VI we outline possible future developments.

II. THE PROBLEM

The complexity of the problem of partitioning a graph into Hamiltonian subgraphs strongly depends on the constraints imposed on the size of the subgraphs considered. For example, when no conditions are imposed on the size of the subgraphs, standard matching techniques find a partition in polynomial time [19]. However, when the subgraphs of the partition are required to have a cardinality greater than or equal to K , with $K \geq 3$, the problem becomes NP-complete [1]. In this paper we consider the $K = 3$ problem, that can be formulated as follows: *given a directed graph without self-loops $G = (V, E)$ where V is the set of vertices and E the set of edges, can the ver-*

tices be partitioned into disjoint sets V_1, V_2, \dots, V_k for some k such that each V_i contains at least three vertices and induces a subgraph G that contains a Hamiltonian cycle?

Figure 1 illustrates the problem for a graph composed of a set of $N_V = 7$ vertices $V = \{1, \dots, 7\}$, and $N_E = 11$ edges $E = \{(1, 2), (2, 5), (2, 6), (3, 4), (4, 3), (4, 7), (5, 1), (5, 6), (6, 3), (6, 7), (7, 6)\}$ (Fig. 1a). A solution exists for this graph because it does have a partition into Hamiltonian subgraphs with one cycle of length three $V_1 = \{1, 2, 5\}$, and one cycle of length four $V_2 = \{3, 4, 6, 7\}$ (Fig. 1b). We stress that, since the problem requires the cycle length to be at least three, the cycles of length two do not appear in the solution.

This problem can be tackled by associating to each edge $(i, j) \in E$ a binary variable $x_{ij} \in \{0, 1\}$, that equals 1 when vertices i and j are connected in the solution (see green arrows in Fig. 1b), 0 otherwise. We note that since the number N_E of existing edges is in general smaller than the number $N_V(N_V - 1)$ of possible edges among all the vertices, associating variables x_{ij} only to the existing edges makes the size of the problem as small as possible.

One can then formulate the problem as:

$$\text{maximise } \sum_{ij} x_{ij} \quad (1)$$

subject to the following constraints:

$$\sum_{ij} x_{ij} = N_V, \quad (2)$$

$$\sum_j x_{ij} \leq 1 \quad \forall i \in V, \quad (3)$$

$$\sum_i x_{ij} \leq 1 \quad \forall j \in V, \quad (4)$$

$$x_{ij} + x_{ji} \leq 1 \quad \forall (i, j), (j, i) \in E. \quad (5)$$

Constraint (2) guarantees that the number of edges is equal to the number of vertices. Constraint (3) guarantees that for every vertex there is no more than one outgoing edge, likewise does constraint (4) for the incoming edges. Constraints (2)-(4) guarantee that the solution will be a partition into Hamiltonian subgraphs. Finally, constraint (5) ensures that two vertices can be connected to each other by maximum one edge, meaning that cycles of length two are forbidden.

III. QUBO FORMULATION

The optimisation problem described by Eqs. (1)-(5) can be rewritten using the QUBO formalism, which is suitable for a quantum annealer [20]. In the QUBO formalism we look for a configuration \mathbf{x} , where \mathbf{x} is a vector with components x_{ij} , that minimizes the following cost function:

$$J(\mathbf{x}) = F(\mathbf{x}) + P(\mathbf{x}). \quad (6)$$

The first term of Eq. (6) is

$$F(\mathbf{x}) = - \sum_{ij} x_{ij} \quad (7)$$

and corresponds to Eq. (1).

The second term of Eq. (6) is a penalty term

$$P(\mathbf{x}) = P_{\text{out}}(\mathbf{x}) + P_{\text{in}}(\mathbf{x}) + P_{\text{no pairs}}(\mathbf{x}), \quad (8)$$

where

$$P_{\text{out}}(\mathbf{x}) = \sum_i a_i \sum_{j, j' > j} x_{ij} x_{ij'} \quad (9)$$

$$P_{\text{in}}(\mathbf{x}) = \sum_j b_j \sum_{i, i' > i} x_{ij} x_{i'j} \quad (10)$$

$$P_{\text{no pairs}}(\mathbf{x}) = c \sum_{i, j > i} x_{ij} x_{ji} \quad (11)$$

The quantities in Eqs. (9)-(11) implement the constraints of Eqs. (3), (4) and (5), given that they will be zero when the configuration \mathbf{x} is allowed and positive when the constraint is violated, thus penalising forbidden configurations. Equations (9)-(11) are based on the fact that for any two binary variables y and z , the constraint $y + z \leq 1$ is equivalent to $y \cdot z = 0$. We note that it is not necessary to encode constraint (2) as a penalty term, since it has the same functional form as Eq. (1), and checking the solution found will be sufficient.

When translating the constraints into penalties one needs to choose the penalty constants a_i, b_j, c large enough compared to the strength of the term $\sum_{ij} x_{ij}$. However, due to the hardware implementation, these cannot be chosen arbitrarily large. An optimal choice for the penalty constants is presented in Appendix A.

IV. IMPLEMENTATION ON A QUANTUM ANNEALER

A. Quantum annealing

The constructed QUBO problem is solved on a D-Wave Advantage quantum annealer, containing 5436 physical working qubits. The starting point for the quantum routine used is a quantum state that corresponds to the ground state of a drive Hamiltonian

$$H_0 = - \sum_{\ell} \sigma_{\ell}^x. \quad (12)$$

This Hamiltonian is slowly changed to the problem Hamiltonian H_1 whose ground state represents the state with lowest energy for the QUBO problem. Its general form is that of an Ising-like Hamiltonian:

$$H_1 = \sum_{\ell} h_{\ell} \sigma_{\ell}^z + \sum_{\ell \ell'} t_{\ell \ell'} \sigma_{\ell}^z \sigma_{\ell'}^z. \quad (13)$$

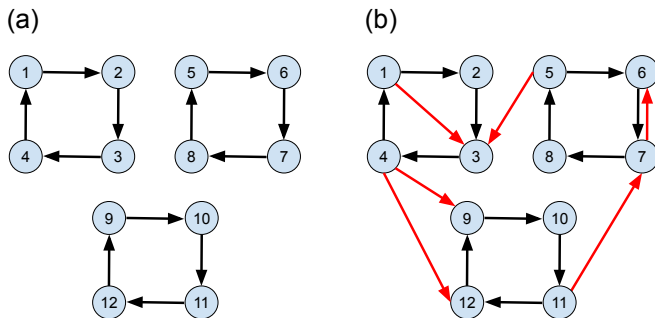


FIG. 2. **Construction of the input graphs for the partitioning problem.** (a) An example of graph G_0 with parameters $n = 3$, $L = 4$, and an equal number of vertices and edges $N_V = N_E = 12$. (b) A graph G generated from G_0 , by adding $N_{\text{noise}} = 6$ new edges (red arrows). For G we have $N_V = 12$, $N_E = 18$.

In H_0 and H_1 , ℓ and ℓ' are indices denoting the position of the physical qubits in the hardware, $\sigma_\ell^{x,z}$ are Pauli operators, and the parameters h_ℓ and $t_{\ell\ell'}$ are set by the QUBO problem.

The total evolution can then be modelled via the Hamiltonian $H(s) = A(s)H_0 + B(s)H_1$, where $A(s)$ and $B(s)$ are a decreasing and increasing function of the dimensionless schedule parameter $s \in [0, 1]$, respectively. The $A(s)$ and $B(s)$ functions are fixed by the hardware, while the time variation of s is controlled by the programmed schedule. In our experiment we use a schedule having a total duration of $300 \mu\text{s}$, composed of an initial annealing where the parameter s is linearly ramped up from 0 to 0.4 in $80 \mu\text{s}$, followed by a pause at $s = 0.4$ lasting for $100 \mu\text{s}$, and a second part of the annealing consisting of a linear ramp of s from 0.4 to 1 in $120 \mu\text{s}$.

The mapping of the QUBO problem in Eq. (6) to the Ising-like Hamiltonian in Eq. (13) is done by identifying the two states $\{0, 1\}$ of the variables x_{ij} with the two eigenstates of the σ_ℓ^z operator of the qubit ℓ . Since the physical qubits in the quantum processor are not fully connected to each other, each logical qubit is embedded into a chain of one or more physical qubits. To find such an embedding, we use the *minorminer* algorithm [21] provided by D-Wave, with its default parameters.

B. Protocol for solving the partitioning problem

In this section we present the steps for the protocol we use to solve the problem on the quantum annealer: (i) graph construction, (ii) problem submission, (iii) check of the output.

Algorithm 1 Solution check. The pseudocode describes the function used to verify whether a graph $G' = (V, E')$, with $E' \subseteq E$, is a partition of a graph $G = (V, E)$ into Hamiltonian subgraphs with three or more vertices.

Input: Graphs $G' = (V, E')$ and $G = (V, E)$

Output: True if G' is a partition of G into Hamiltonian subgraphs with three or more vertices, False otherwise

Procedure:

```

1: repeat
2:   Initialise two empty sets  $C_V = \{\}$  and  $C_E = \{\}$ 
3:   Pick a vertex  $v_{\text{start}} \in V$ 
4:   Assign  $v_{\text{from}} := v_{\text{start}}$ 
5:   repeat
6:     Find the edges  $E_{\text{from}} \subseteq E'$  going out of  $v_{\text{from}}$ 
7:     if  $E_{\text{from}}$  has exactly one element then
8:       Add the vertex  $v_{\text{from}}$  to  $C_V$ 
9:       Add the edge  $e$  in  $E_{\text{from}}$  to  $C_E$ 
10:    else
11:      return False
12:    end if
13:    Assign  $v_{\text{to}}$  to the vertex pointed at by  $e$ 
14:    if ( $v_{\text{to}} \neq v_{\text{start}}$ ) and ( $v_{\text{to}} \in C_V$  or  $C_E = E'$ ) then
15:      return False
16:    end if
17:    Assign  $v_{\text{from}} := v_{\text{to}}$ 
18:  until  $v_{\text{to}} = v_{\text{start}}$ 
19:  if  $C_V$  has exactly 2 elements then
20:    return False
21:  else if  $C_V$  has 3 elements or more then
22:    Remove from  $V$  the vertices contained in  $C_V$ 
23:    Remove from  $E'$  the edges contained in  $C_E$ 
24:  end if
25: until no vertices are left in  $V$  and no edges are left in  $E'$ 
26: return True

```

(i) We start by generating a graph G_0 composed of n disjoint cycles of length L (Fig. 2a). This contains nL vertices and nL edges. A new graph G is generated starting from G_0 , by introducing noise, i.e. adding N_{noise} new randomly chosen edges that connect the existing vertices (Fig. 2b). The so-constructed graph G will always admit G_0 as solution, even though additional solutions might also appear when the amount of noise is large.

(ii) The graph G is then transformed into a QUBO problem as explained in the previous sections and submitted to the quantum annealer. The annealing schedule is run 100 times, and the frequency of the final states obtained is computed.

(iii) Using Algorithm 1 we check if the lowest energy state (or states in the degenerate case) corresponds to a partition of G into Hamiltonian subgraphs containing cycles of length three or more. If that is the case, the probability P_{sol} of finding a solution is equal to frequency of the lowest energy state (or the sum of the frequencies of the lowest energy states in the degenerate case), if not $P_{\text{sol}} = 0$. We note that the solution check algorithm runs in polynomial time. The only step that is proportional to the size of the problem is line 6 in Algorithm 1, which is a $\mathcal{O}(N_E)$. That step is executed at maximum N_V times, which makes the overall algorithm a $\mathcal{O}(N_E N_V)$.

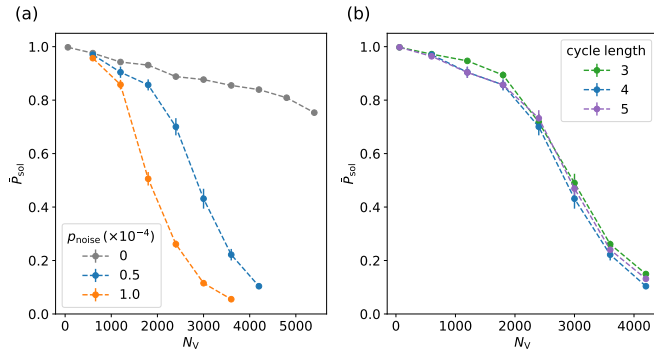


FIG. 3. **Single-run solution probability as a function of the number of vertices.** (a) \bar{P}_{sol} is shown as a function of N_V for cycles of length 4 for different p_{noise} . For all curves the probability to find a solution in a single run on the quantum annealer decreases as the system size increases. With noise, the dependence on the system size is stronger: for $N_V = 4200$ and $p_{\text{noise}} = 0.5 \times 10^{-4}$ (i.e. $N_{\text{noise}} = 882$) the probability is $\bar{P}_{\text{sol}} = 0.104(9)$, and for $N_V = 3600$ and $p_{\text{noise}} = 1 \times 10^{-4}$ (i.e. $N_{\text{noise}} = 1295$), the probability is $\bar{P}_{\text{sol}} = 0.055(8)$. (b) \bar{P}_{sol} is shown as a function of N_V for $p_{\text{noise}} = 0.5 \times 10^{-4}$ for different cycle lengths. The probability exhibits the same behaviour as a function of the problem size regardless of the cycle length used in the input graph configuration. In both panels, the error bars show the standard error on the mean.

To collect statistics on P_{sol} , we repeat the steps (i) to (iii) 50 times and average P_{sol} over the 50 repetitions to obtain \bar{P}_{sol} , that represents the average probability to find a solution with a single run (i.e. a single annealing schedule) on the quantum annealer.

V. RESULTS

We start by fixing the fraction p_{noise} of the maximum allowed number of additional edges for the given number of vertices N_V , and set $N_{\text{noise}} = \text{round}(p_{\text{noise}} N_V (N_V - 2))$. In the simplest scenario, i.e. $p_{\text{noise}} = 0$, the quantum annealer easily finds a solution regardless of the problem size (grey points in Fig. 3a). Even when considering a problem with a very large number of vertices and edges, $N_V = N_E = 5400$, where the graph size is very close to the total number of working physical qubits available (5436), the probability to find a solution with a single run on the quantum annealer is $\bar{P}_{\text{sol}} = 75(1)\%$. We observe that \bar{P}_{sol} decreases with N_V with a slope that strongly depends on p_{noise} , and the quantum annealer finds a solution up to $N_V = 4200$ for $p_{\text{noise}} = 0.5 \times 10^{-4}$ and up to $N_V = 3600$ for $p_{\text{noise}} = 1 \times 10^{-4}$ (blue and orange points in Fig. 3a).

Figure 3b shows that the single-run solution probability \bar{P}_{sol} does not depend on the cycle length. This can be explained by the fact that the dimension of the combinatorial space depends on the number of all the possible paths in the input graph, which is determined only by

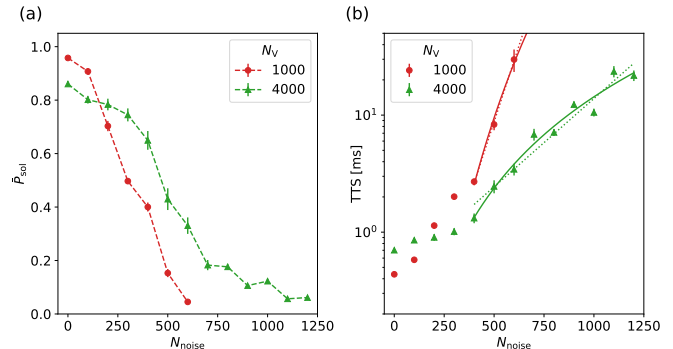


FIG. 4. **Single-run solution probability and time to solution as a function of the number of added random edges.** (a) \bar{P}_{sol} is shown as a function of N_{noise} for cycles of length 4 and different N_V . The single-run solution probability decreases as the number of random edges becomes larger. For larger sizes of the problem, \bar{P}_{sol} goes to zero more slowly. (b) TTS shown for the same points as panel (a). The dotted lines show exponential fits to the data in the range $N_{\text{noise}} \geq 400$ with equation $\log(\text{TTS}/1\text{ms}) = a + bN_{\text{noise}}$ and the solid lines show power law fits with equation $\log(\text{TTS}/1\text{ms}) = a + b \log(N_{\text{noise}})$.

N_V and p_{noise} .

To further investigate the dependence on the combinatorial complexity, we now fix the number of vertices N_V and vary the number of added edges N_{noise} . To give an intuition on how the complexity of the problem scales with N_{noise} , we can think of a classical approach based on Algorithm 1. Without any edges added, there is only one possible simple path. When we add one edge of noise, there will be one vertex with two outgoing edges: this bifurcation gives rise to two different simple paths. Each of them could be then fed into Algorithm 1 to check whether it is a solution. However, when the number of added edges increases, the number of simple paths to be checked can be up to $2^{N_{\text{noise}}}$, and therefore finding a solution with this classical procedure becomes exponentially hard.

In Fig. 4 we show the results obtained with the quantum annealer. For a small amount of added edges ($N_{\text{noise}} \lesssim 100$) the single-run solution probability is higher for the smaller system size explored (Fig. 4a). However, as N_{noise} is increased, for a given number of added edges it becomes easier to find a solution for a system where the size is larger. We note that, regardless of the value of the single-run solution probability, the same problem can be submitted multiple times in order to find a solution at least once with arbitrarily high probability. Fixing the desired probability to 99%, the time needed to find a solution is given by [22]

$$\text{TTS} = (t_{\text{anneal}} + t_{\text{pause}}) \frac{\log(1 - 0.99)}{\log(1 - \bar{P}_{\text{sol}})}, \quad (14)$$

where the first term is the single-run time (i.e. the sum of the times used in the schedule of the quantum annealer

	a	b
power law fit $N_V = 1000$	-34(3)	5.9(6)
power law fit $N_V = 4000$	-15(1)	2.6(2)
exponential fit $N_V = 1000$	-3.8(2)	0.0120(4)
exponential fit $N_V = 4000$	-0.8(3)	0.0035(3)

TABLE I. **Fit parameters.** The table reports the parameters obtained from the fits to the data shown in Fig. 4b. For the exponential fit, the parameter b is much less than $\log 2$, expected for the $2^{N_{\text{noise}}}$ classical scaling described in section V.

$t_{\text{anneal}} = 200 \mu\text{s}$ and $t_{\text{pause}} = 100 \mu\text{s}$) and the second term is the number of necessary runs to find a solution with the desired probability.

In Fig. 4b we show the behaviour of the time to solution TTS as a function of the number of added random edges. We fit the large N_{noise} behaviour of TTS with an exponential and power law functions. The fit parameters are reported in Table I. It is clear from the plots that for the range explored TTS is compatible with either fit. However, even in the exponential case, the scaling is much slower than the one of the classical procedure explained earlier, that scales as $\exp(N_{\text{noise}} \log 2)$.

VI. OUTLOOK

Possible extensions of the problem presented here can be considered for graphs where weights are assigned to the edges, or where different constraints on the cycle length are present.

We point out that, if self-loops are included in the construction of the problem and the constraint on the cycle length is lifted, our method could be used to compute the permanent of a matrix, since finding all the cycle covers of a graph is equivalent to computing the permanent of its adjacency matrix [23].

Additional information: The code used to generate the results presented in this paper is available at https://github.com/quantumglare/quantum_cycle. Further information can be requested at info@quantumglare.com.

Appendix A: Constraints

In order to properly set the penalty constants in Eqs. (9)-(11) we proceed with an analysis of the different cost terms in Eq. (6), that allows us to choose the penalty constants as small as possible.

We require the cost $J(\mathbf{x}_a)$ of an allowed configuration \mathbf{x}_a that satisfies all constraints to be lower than the

cost $J(\mathbf{x})$ of any configuration \mathbf{x} that violates at least one constraint, i.e.

$$J(\mathbf{x}) > J(\mathbf{x}_a) \quad \forall \mathbf{x}, \mathbf{x}_a. \quad (\text{A1})$$

Let us first consider the constraint on the number of outgoing edges given in Eq. (3), whose corresponding penalty is given in Eq. (9). Any configuration that violates only that constraint can be decomposed as $\mathbf{x} = \mathbf{x}_a + \mathbf{x}'$, where \mathbf{x}' is a vector whose only elements equal to 1 are those corresponding to the additional edges. From equation (A1) it follows that, for every vertex i ,

$$a_i \sum_{j,j'>j} x_{ij}x_{ij'} > \sum_j x'_{ij}. \quad (\text{A2})$$

Equation (A2) is satisfied by setting:

$$a_i = \max_{\mathbf{x}, \mathbf{x}'} \left(\frac{\sum_j x'_{ij}}{\sum_{j,j'>j} x_{ij}x_{ij'}} \right) + \epsilon, \quad (\text{A3})$$

where ϵ is an arbitrarily small positive constant, which makes a_i an optimal choice. The number $N_{\mathbf{x}',i}$ of non-zero elements in \mathbf{x}' varies from 1 to the total number $N_{\text{out},i}$ of outgoing edges from vertex i in the original graph. In terms of $N_{\mathbf{x}',i}$ Eq. (A3) becomes

$$a_i = \max_{N_{\mathbf{x}',i}} \left(\frac{N_{\mathbf{x}',i}}{\binom{N_{\text{out},i}}{N_{\mathbf{x}',i}}} \right) + \epsilon \quad (\text{A4})$$

where in the denominator the round brackets denote the binomial coefficient. The maximum is achieved for $N_{\mathbf{x}',i} = 1$, giving $a_i = 1 + \epsilon$ for all vertices i of the graph that might violate the constraint. For all other vertices we simply set it to zero, leading to

$$a_i = \begin{cases} 1 + \epsilon & \text{if } N_{\text{out},i} > 1, \\ 0 & \text{otherwise.} \end{cases} \quad (\text{A5})$$

Likewise, for the constraint on the number of ingoing edges in Eq. (4), which corresponds to the penalty in Eq. (10), we set

$$b_i = \begin{cases} 1 + \epsilon & \text{if } N_{\text{in},i} > 1, \\ 0 & \text{otherwise,} \end{cases} \quad (\text{A6})$$

where $N_{\text{in},i}$ is the number of ingoing edges to vertex i in the original graph.

A similar reasoning for the constraint to forbid pairs in Eq. (5), which corresponds to the penalty in Eq. (11), leads to

$$c = 2 + \epsilon. \quad (\text{A7})$$

-
- [1] D. S. J. Michael R. Garey, *Computer and intractability: a guide to the theory of NP-completeness*, A Series of books in the mathematical sciences (W. H. Freeman and Co Ltd, 1979).
- [2] D. Venturelli, D. J. J. Marchand, and G. Rojo, arXiv e-prints (2015), [1506.08479 \[quant-ph\]](#).
- [3] F. Neukart, G. Compostella, C. Seidel, D. von Dollen, S. Yarkoni, and B. Parney, arXiv e-prints, arXiv:1708.01625 (2017), [arXiv:1708.01625 \[quant-ph\]](#).
- [4] T. Stollenwerk, B. O’Gorman, D. Venturelli, S. Mandrà, O. Rodionova, H. K. Ng, B. Sridhar, E. G. Rieffel, and R. Biswas, arXiv e-prints (2017), [arXiv:1711.04889 \[quant-ph\]](#).
- [5] D. Inoue, A. Okada, T. Matsumori, K. Aihara, and H. Yoshida, arXiv e-prints (2020), [arXiv:2003.07527 \[math.OC\]](#).
- [6] T. Stollenwerk, E. Lobe, and M. Jung, arXiv e-prints (2018), [arXiv:1811.09465 \[quant-ph\]](#).
- [7] G. Bass, C. Tomlin, V. Kumar, P. Rihaczek, and I. Dulny, Joseph, *Quantum Science and Technology* **3**, 024010 (2018), [arXiv:1709.05381 \[quant-ph\]](#).
- [8] A. Perdomo-Ortiz, N. Dickson, M. Drew-Brook, G. Rose, and A. Aspuru-Guzik, *Scientific Reports* **2**, 571 (2012).
- [9] D. Venturelli and A. Kondratyev, *Quantum Machine Intelligence* **1**, 17 (2019).
- [10] J. Cohen, A. Khan, and C. Alexander, arXiv e-prints (2020), [arXiv:2007.01430 \[q-fin.GN\]](#).
- [11] Y. Ding, L. Lamata, J. D. Martín-Guerrero, E. Lizaso, S. Mugel, X. Chen, R. Orús, E. Solano, and M. Sanz, “Towards prediction of financial crashes with a d-wave quantum computer,” (2019), [arXiv:1904.05808 \[quant-ph\]](#).
- [12] M. Constantino, X. Klimentova, A. Viana, and A. Rais, *European Journal of Operational Research* **231**, 57 (2013).
- [13] S. Luo and P. Tang, in *Proceedings of the 24th International Conference on Artificial Intelligence*, IJCAI’15 (AAAI Press, 2015) pp. 209–215.
- [14] R. Anderson, I. Ashlagi, D. Gamarnik, and A. E. Roth, *Proceedings of the National Academy of Sciences* **112**, 663 (2015).
- [15] A. Abdulkadiroglu and T. Sönmez, *Journal of Economic Theory* **88**, 233 (1999).
- [16] T. Sönmez and T. B. Switzer, *Econometrica* **81**, 451 (2013).
- [17] W. Fang, P. Tang, and S. Zuo, in *Proceedings of the Twenty-Fifth International Joint Conference on Artificial Intelligence, IJCAI 2016, New York, NY, USA, 9–15 July 2016*, edited by S. Kambhampati (IJCAI/AAAI Press, 2016) pp. 264–270.
- [18] M. Bläser and B. Siebert, in *Algorithms — ESA 2001*, edited by F. M. auf der Heide (Springer Berlin Heidelberg, Berlin, Heidelberg, 2001) pp. 368–379.
- [19] J. Edmonds and E. L. Johnson, “Matching: A well-solved class of integer linear programs,” in *Combinatorial Optimization — Eureka, You Shrink!: Papers Dedicated to Jack Edmonds 5th International Workshop Aussois, France, March 5–9, 2001 Revised Papers*, edited by M. Jünger, G. Reinelt, and G. Rinaldi (Springer Berlin Heidelberg, Berlin, Heidelberg, 2003) pp. 27–30.
- [20] F. Glover, G. Kochenberger, and Y. Du, “A tutorial on formulating and using qubo models,” (2019), [arXiv:1811.11538 \[cs.DS\]](#).
- [21] J. Cai, W. G. Macready, and A. Roy, arXiv e-prints, arXiv:1406.2741 (2014), [arXiv:1406.2741 \[quant-ph\]](#).
- [22] T. Albash and D. A. Lidar, *Phys. Rev. X* **8**, 031016 (2018).
- [23] T. Rudolph, *Phys. Rev. A* **80**, 054302 (2009).